

Material damage in space from microparticle impact

L. BERTHOUD

European Space Agency, Materials and Processes Division, ESTEC, Postbus 299, 2200 AG Noordwijk, The Netherlands

J.C. MANDEVILLE

CERT-ONERA, Department of Space Technology 2Av. E. Belin, 31055 Toulouse cedex, France

A large variety of materials have now been recovered from long term exposure to the space environment. The authors have investigated samples which have spent several years in space on various satellites, including: the NASA satellite 'Long Duration Exposure Facility', the Franco–Russian 'Aragatz' mission experiment on MIR and the Hubble Space Telescope. The samples come mainly from experiments devoted to the study of meteoroids and orbital debris and the damage that these can cause to spacecraft materials. In this paper some interesting impact features have been selected to demonstrate the different types of damage sustained on different materials.

1. Introduction

Space is a hostile environment. Spacecraft have to be designed to cope with high vacuum, ultra-violet (UV) radiation, protons and electrons trapped in the Van Allen radiation belts, atomic oxygen, thermal cycling and meteoroid and debris impact. In this paper we concentrate mainly on particle impact and the combined effects of the other threats. All large spacecraft with a mission duration of more than a few days are susceptible to impacts occurring at extremely high speeds or 'hypervelocities'. These can make craters or punch holes in flight-critical systems, leading to catastrophic failure.

In the past, many experimental studies of the degradation of materials in space were carried out by ground simulation tests. These, together with theoretical investigations, have shown that impact mechanisms at 'hypervelocities' (velocities greater than 6 km s^{-1}) can largely be explained using shock wave physics and hydrodynamic theory. However, in the last few years a large variety of materials have been recovered from space itself. The analysis of these is being carried out in laboratories throughout Europe and the United States and forms the basis of this study.

2. Flight samples

The materials discussed here come from three sources: the Russian space station MIR, the NASA satellite LDEF and the Hubble Space Telescope repair mission.

2.1. MIR

The MIR space station has been in orbit at an altitude of 350–450 km with an inclination of 51.6° since

February 1986. The French experiment 'Echantillons' was placed outside the station during the Franco–Russian mission 'Aragatz' (see Fig. 1). It was deployed on the 9th December 1988 and recovered thirteen months later [1]. The material samples consisted mainly of pieces of aluminium foil and glass.

2.2. LDEF

The NASA Long Duration Exposure Facility (LDEF) was launched into a 482 km altitude orbit from the payload bay of the Space Shuttle Challenger in April 1984 (Fig. 2). It was retrieved from orbit by Shuttle Columbia after 5.7 years [2]. The materials examined here include copper, Mylar, Kapton, Teflon, glass and aluminium. They were part of the French Cooperation Payload 'FRECOPA', which was mounted on the trailing surface of the satellite [3].

2.3. HST

The Hubble Space Telescope was launched on the 24th April 1990 into a 614 km LEO orbit (Fig. 3). During the Hubble repair mission in December 1993, one of its two roll-out solar arrays was retracted and brought back to Earth [4]. This provided solar cells and thermal insulation material for investigation.

3. Experimental procedure

Optical microscopes, including a CCD video microscope, were used for an initial scan of the specimens. This revealed the general state of the specimen surface and the larger features. The transmission mode was particularly useful for spotting perforations. Scanning

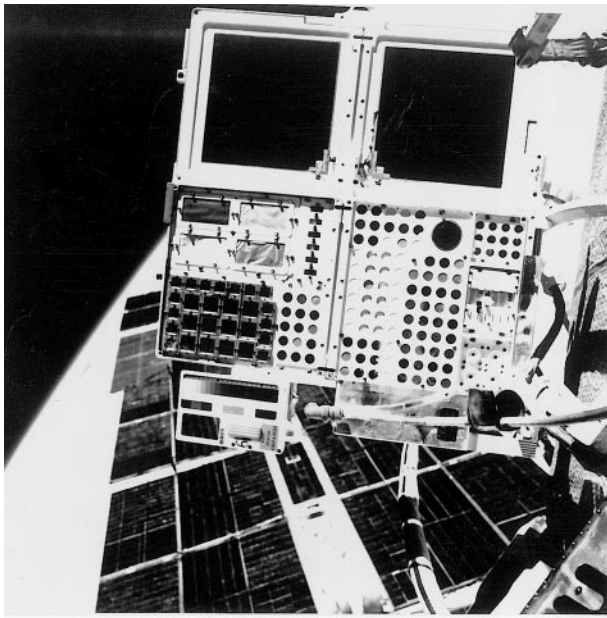


Figure 1 The echantillons module mounted on the side of the MIR space station.

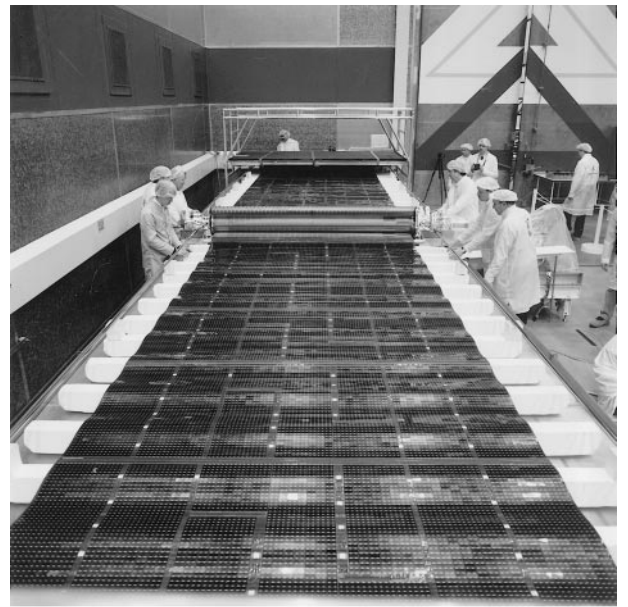


Figure 3 The Hubble Space Telescope solar array being rolled out at Matra Marconi Space, Bristol after its retrieval.



Figure 2 The LDEF satellite above the Shuttle cargo bay.

electron microscopes (SEM) were then used for detailed investigation of the features. These, and other techniques, have already been used successfully in examination of space surfaces [5].

The distinctive morphology of craters (Fig. 4) should make them easy to distinguish from material defects and contamination. However, in practice, SEM examination of exposed surfaces was ham-

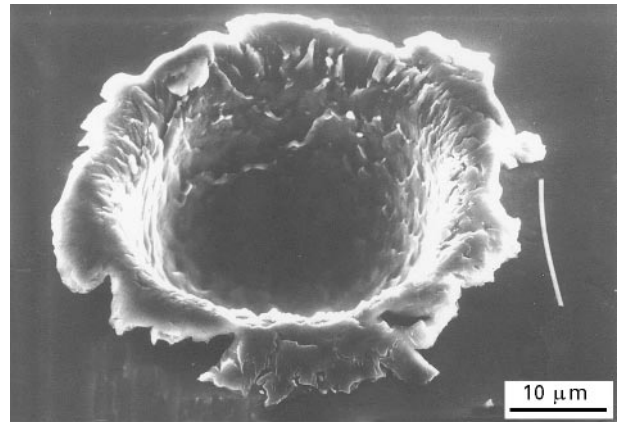


Figure 4 SEM image of the impact crater in an LDEF aluminium sample (diameter is 120 µm).

pered by the reduced resolution and charging caused by defects, contamination and oxidized surfaces.

4. Impacts on different materials

4.1. Aluminium

A typical impact crater found in aluminium is shown in Fig. 4. Craters on ductile surfaces are characterized by a radial symmetry, a raised lip and a dark central cavity or pit. Perforations look similar to craters except on the very thinnest of targets, where the hole usually has little lip and takes on the same shape as the impacting particle. Most of the work on particle-target interaction models has been done with aluminium as a target [6], although glass has been the subject of some investigations [7]. Very little is known about the relative sizes of damage to materials such as Mylar, Kapton and tefloned glass fibre.

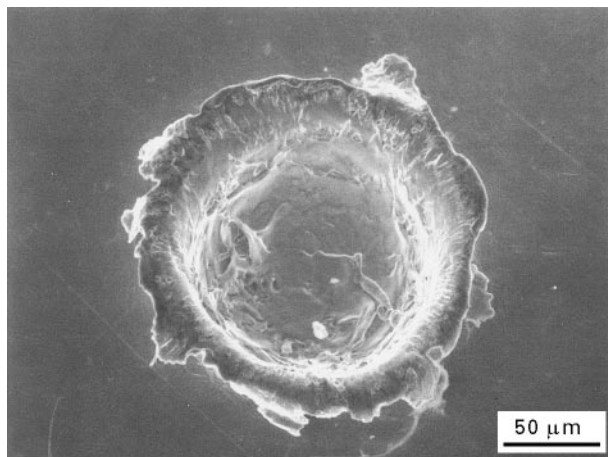


Figure 5 SEM image of crater on LDEF copper sample A3-2 (diameter is 110 μm).

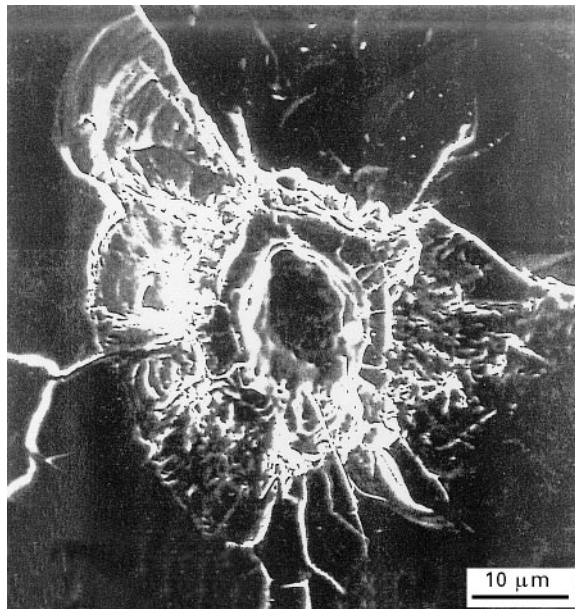


Figure 6 SEM image of the impact in a glass sample from LDEF (central pit diameter = 48 × 34 μm).

4.2. Copper

Only one 110 μm-sized impact feature was found on the copper sample, which is shown in Fig. 5. The morphology of the impact was very similar to those found on aluminium; namely a radial symmetry, a raised lip and melt 'walking' up the crater walls. The depth to diameter ratio of the crater was measured to be 0.43 which is shallower than the average value of 0.55 in aluminium. This difference is possibly due to the higher density of copper.

4.3. Glass

Fig. 6 shows an example of an impact on a quartz glass sample on LDEF. An asymmetrical area is visible around the central pit, where material has been ejected by the rarefaction shock wave returning to the surface (a process called 'spallation'). The central pit measures 34 × 48 μm and has a thin lip. The rounded

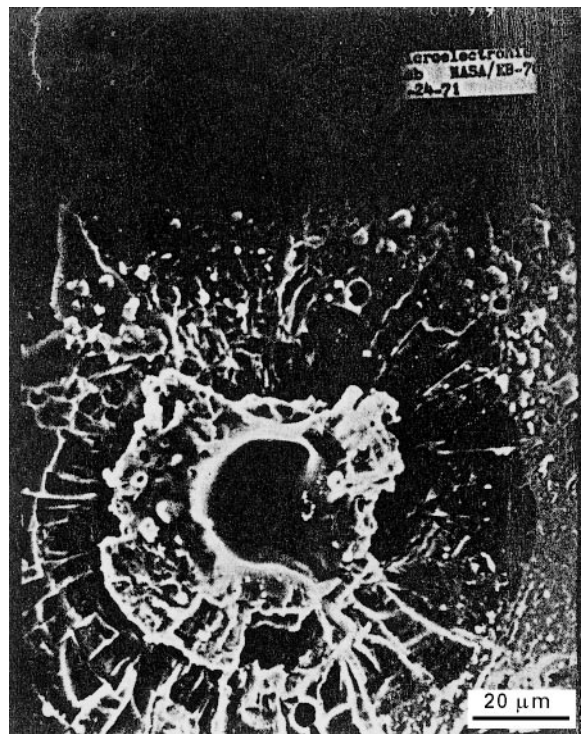


Figure 7 SEM image of the crater formed by the impact of micro-meteoroids on a glassy sphere from the Moon's surface brought back by Luna 16 (photo from NASA JSC, Houston).

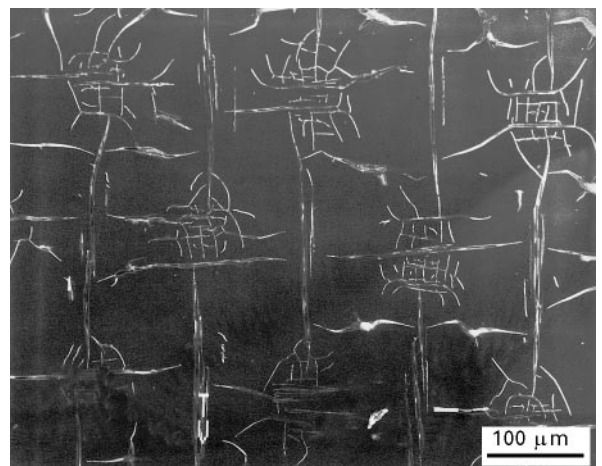


Figure 8 The regular pattern of microcracks covering LDEF thermal blankets.

contours inside the pit indicate that the glass has softened (glass softens around 1100–1400 °C). For comparison, Fig. 7 shows a crater formed in a lunar rock, as the Moon is also pitted by craters from a continual rain of meteoroids. The crater formed on the glassy material of the rock shows a similar morphology to those on the space samples.

4.4. Thermal covers

Protective thermal covers consisting of tefloned glass fibre with aluminized mylar for the FRECOPA power supply were examined. A regular pattern of microcracks was found, which was not present on reference samples (shown in Fig. 8). The teflon matrix seems to have been eroded away by radiation and atomic

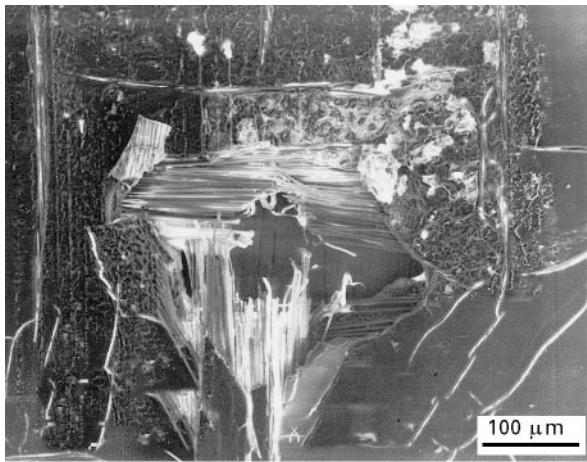


Figure 9 Impact found on the LDEF thermal blanket (perforation diameter = 200 μm).

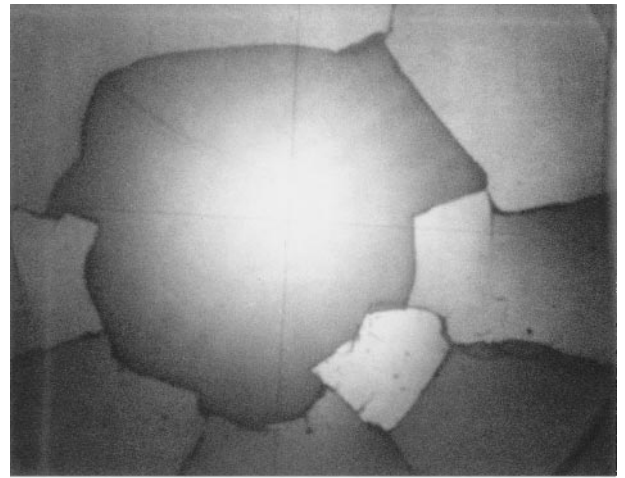


Figure 11 Angular fracture produced in mylar (Diameter = $1.8 \times 1.5 \text{ mm}$).

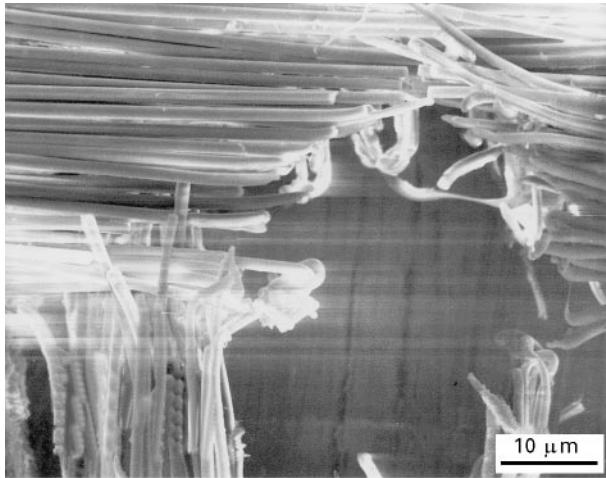


Figure 10 Detail of the LDEF thermal cover impact showing fusion products on fibre ends.

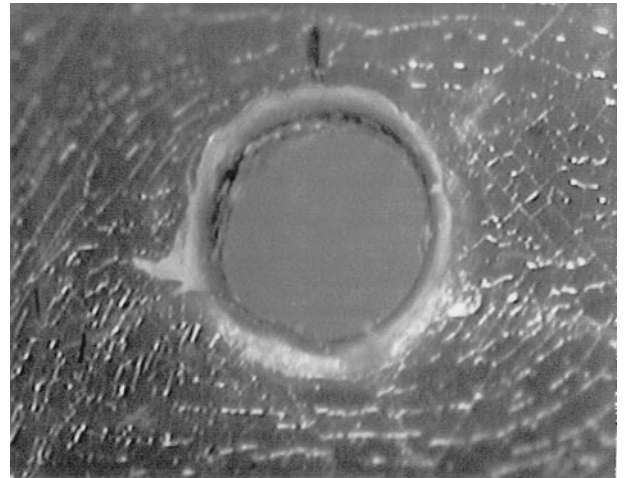


Figure 12 Perforation of Kapton tape on MIR (Diameter = 180 μm).

oxygen to a point well beneath the substrate surface. Wider fissures occurred in parts of the matrix unsupported by glass fibre tissue, sometimes perforating the matrix completely. Fig. 9 shows a perforation of 200 μm diameter in the tefloned glass. The damage was limited on the left side and above and below by neighbouring bunches of fibres. An area of 500 μm diameter of the top layer of teflon was fractured along microcracks present before impact. Fig. 10 – a detail of Fig. 9 – shows evidence of fibre fracture and melting (rounded fusion products).

The aluminized mylar was degraded in two ways by space exposure. Firstly the aluminium coating turned a goldish colour on the side exposed to the sun, due to contamination. And secondly, the mylar became brittle and tore easily with handling. This is a known effect of radiation on certain polymers; the radiation causes crosslinking of the chains and embrittlement ensues. A perforation was left by the passage of the same microparticle which caused the above impact. The perforation was significantly larger than that produced in the tefloned glass fibre. Fig. 11 shows the angular fracture. Cracks radiate outward from the impact point.

4.5. Kapton tape

As is shown in Fig. 12 an impact measuring 180 μm in diameter was found in a sample of Kapton tape 50 μm thick. The tape was perforated and showed signs of fusion on the lip. Black markings were found on the surface behind the tape. These were thought to have been caused by carbonization of the tape upon impact. Charring of Kapton occurs at temperatures above 800 $^{\circ}\text{C}$.

4.6. HST solar cell on flexible blanket substrate

Hubble space telescope solar arrays consist of a complex layered structure (Fig. 13). Since the top layer is a piece of glass, the smaller craters resemble those in glass surfaces. Larger particles penetrate through the various layers to different depths, exposing the layers as they go through. Each layer slows the impacting particle at a different rate, making interpretation of the larger craters difficult [8]. 148 particles punched right through the 710 μm thick array from both sides

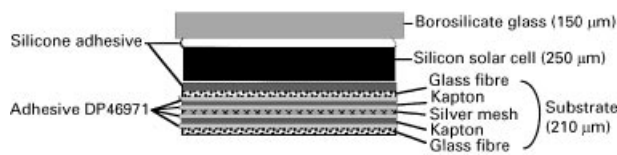


Figure 13 Section through an HST solar cell mounted on its substrate.

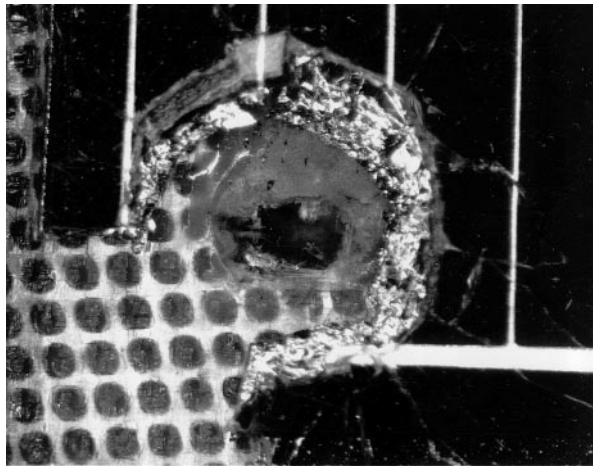


Figure 14 Optical microscope image of perforated HST cell (diameter of outer damage is 3.1 mm).

(the area of each side was approx. 20 m^2). An optical microscope image of one of these perforations is shown in Fig. 14.

5. Results and lessons learnt from flight experiments

Even when there is no trace of the impact particle left in a crater, it is possible to deduce its size, density, shape and impact angle from the morphology of the crater. For example, to estimate the diameter of a particle, the diameter of its impact is measured and an empirical equation based on laboratory simulations can be used to convert this to the particle diameter. This data is described in detail elsewhere [9, 10].

One of the major lessons learnt from this work is that not only experimental surfaces, but also frames, clamps and thermal blankets can be used as particle detectors. To make best use of such impact information, these surfaces should be calibrated with ground simulation experiments before flight. We have seen that damage to materials depends to a large extent upon target properties. Upon impact, ductile materials, such as aluminium and copper, undergo plastic yielding and pure fluid flow if the energy is sufficient to cause melting. Shallower craters will be formed in denser materials. Brittle materials fracture and spall under impact. They will also soften and flow if impact pressures are sufficient. Damage areas are greater in glasses and ceramics than in metals for the same size particle, due to the spalling and cracking (this also makes them more visible). Damage areas on polymers are also larger than on metals, particularly if there has

been embrittlement due to UV exposure. But they are not as large as on glass. Damage on glass fibre weave is often non-circular and difficult to identify, as the shape is determined by the fibre bunches. It also tends to be slightly more extensive than metal damage. For multilayer materials, such as thermal covers, the size of the damage is also a function of its position in the structure (top, 2nd, 3rd layer etc.).

The effect of a major impact on a spacecraft would be catastrophic. But even smaller impacts may cause problems: cratering may affect the thermo-optical properties of a material, and thus the temperature of the equipment; a hole may cause a leak, break a conductive track or expose an underlayer; and impacts may cause a shower of debris to be released, increasing contamination risks. We have also seen that impact effects can be exacerbated by other environmental factors. UV exposure can erode Teflon, embrittle Mylar and Kapton and change the optical properties of aluminium foil. When impacts occur on these weakened zones, greater damage is caused: wider damage areas, deeper penetrations and greater crack propagation around that impact site. One could imagine an impact hole in a satellite that would allow the entry of atomic oxygen, radiation and contaminants, potentially damaging sensitive instruments such as optics.

6. Conclusions

A wide variety of materials exposed to space for several years have been scanned using optical and scanning electron microscopes. Analyses of impacts on the samples reveal useful information about the debris and micrometeoroids which produced them. They also reveal information about the various effects of impacts on different materials. We must now consider not only simple isotropic targets, such as aluminium, but complex multilayer structures, such as composites, thermal blankets and solar arrays. The danger of synergy between the effects of the space environment has also been revealed. An impact on a material already damaged by thermal cycling and UV exposure could provoke a mission-critical incident, whereas individually each type of damage would not constitute a risk.

Acknowledgements

L. Berthoud was supported by an ESA research fellowship during part of this work.

References

1. J. C. MANDEVILLE, *Adv. Space Research* **10** (1990) 397.
2. R. L. O'NEAL and E. B. LIGHTNER, in Proceedings, NASA CP-3134, LDEF First Post-Retrieval Symposium part 1, edited by A.S. Levine, pp 3–48 NASA CP-3134 (NASA, Langley Research Center, Hampton, Virginia, 1991).
3. L. G. CLARK, W. H. KINARD, D. J. GARTER and J. L. JONES (eds) "LDEF Mission 1 Experiments", NASA SP-473, (NASA, Langley, Virginia, 1984).
4. D. EATON, "The HST first servicing mission – a fantastic success," ESA bulletin No. 77, February 1994 (ESTEC, Noordwijk, 1994).
5. C. MIGLIONICO, C. STEIN and L. E. MURR, *J. Mater. Sci.* **26** (1991) 5134.

6. L. BERTHOUD and J. C. MANDEVILLE, "in Proceedings First European Conference on Space Debris", ESOC (European Space Operations Centre) Darmstadt, April 5-7, 1993, edited by W. Flury (ESOC, Darmstadt, 1993).
7. L. BERTHOUD, in Proceedings 6th Int. Symp. on Materials in a Space Environment, ESTEC Noordwijk, September 1994, edited by T. D. Guyenne (ESA, ESTEC, Noordwijk, 1994).
8. J. C. MANDEVILLE, M. RIVAL and C. DURIN, in Proceedings HST Solar Array Workshop, Sept. 1995, ESTEC, Noordwijk, ESA WPP 77, edited by L. Gerlach (ESA, ESTEC, Noordwijk, 1995).
9. J. C. MANDEVILLE and L. BERTHOUD, in Proceedings 'First European Conference on Space Debris', ESOC Darmstadt, April 5-7, 1993, edited by W. Flury (ESOC, Darmstadt, 1993).
10. L. BERTHOUD, J. C. MANDEVILLE, C. DURIN and J. BORG, in 'Proceedings 3rd LDEF Conf. NASA Langley Research Centre VA, November 1993.

*Received 18 August 1995
and accepted 13 February 1996*